The synthesis of a porous-type of TiO$_2$ with rutile structure

Yukiya Yamashita*,**, Kei Ishiguro*, Daisuke Nakai*, Masayoshi Fuji**

*Nippon AEROSIL Co. Ltd., 3 Mita-cho, Yokkaichi, Mie 510-0841, Japan

**Advanced Ceramics Research Center, Nagoya Institute of Technology 3-101-1, Honmachi, Tajimi, Gifu 507-0033, Japan

Abstract

The synthesis of a porous-type of TiO$_2$ with rutile structure was studied. The focuses were on the thermal treatment temperature and time. AEROXIDE® TiO$_2$ P 25, as a fumed TiO$_2$, was thermally treated in a vertical-type tubular furnace by the natural dropping method. Even though the thermal treatment time was less than 1 second, a drastic increase of polymorphism from anatase structure to rutile structure was observed. The relationships between the rutile structure transformation ratio and surface area of obtained porous type of TiO$_2$ were investigated depending on the thermal treatment temperature. The porous-type of fumed TiO$_2$ showed high dispersibility in the sedimentation test although is showed large particle size.

1．Introduction

Titanium dioxide (TiO$_2$) has a wide variety of applications in industrial fields, such as white pigment, ultraviolet cutting and photocatalytic material such as coating, paint, cosmetics,

paper, resin, photocatalytic material and others. Recently, TiO_2 nanomaterials were extensively investigated for their special properties especially focusing on their photocatalytic activities [1].

TiO_2 has three typical crystalline polymorphs, i.e., anatase, brookite and rutile. For industrial purposes, the anatase and rutile structures are mainly used. There are several production processes for industrial applied TiO_2 such as the sulfate process, chloride process, sol-gel process and fumed process. Among these production processes, the fumed process is unique in its production which can produce very fine TiO_2 powders directly from a hydrogen and oxygen burner using the same process as fumed silica [2]. This fumed TiO_2 is composed of weak agglomerated particles like a 3-dimendional network structure and this agglomerate is easily destroyed by the addition of mechanical agitation when it is dispersed in media such as water, organic solvent, resin and others. Due to this unique property, fumed TiO_2 is used as an UV cutting material for cosmetics having a high transparency due to its fine primary particle size. Fumed TiO_2 is a mixture of the anatase and rutile type crystal structures and the main phase being the anatase structure [2]. This material shows excellent photocatalytic activities. Recently, it has been used as a reference material to evaluate photocatalytic activities [3]. However, this excellent photocatalytic activity can also be a disadvantage of fumed TiO_2 in cosmetic applications. Normally, the rutile structure is preferred for this application.

It is well known that anatase transforms into the rutile structure by thermal treatment at a

high temperature. Actually, there are many studies about TiO_2 to prevent or accelerate this transformation. For example, metal oxide additives [4] [5], the addition of SiO_2 [6], the addition of carbon [7], non-metal doping [8] and ultrasonic irradiation as a special processing [9]. However, in general cases, sintering and grain growth of the TiO_2 occur by a thermal treatment, caused a decrease in a dispersibility of the fumed TiO_2. The control of the thermal treatment conditions is very important factor to prevent the sintering and grain growth for the additional thermal treatment.

There are also several studies about sintering of TiO_2 such as microwave irradiation [12], sintering temperature [13], and O_2 pressure [14]. As another approach, the photocatalytic activities have been investigated for the sintered TiO_2 [15]. However, these investigations focused on the production of sintered TiO_2 with a high density. Regarding the fumed TiO2, the increase of the primary particle size depended on the increase of the content of rutile structure was shown depended on rising the thermal treatment temperature to 1000°C for 3 hours [16].

In this current study, it was desired to synthesize a new type of fumed TiO_2 having a high content of rutile and keeping the high dispersiblity by controlling with a partial sintering by the additional thermal treatment at high temperature for very short time. The experimental results suggested that the newly-fumed TiO_2 has a higher porosity in the agglomerate and acts as a porous-type of fumed TiO_2.

2. Experimental details

2.1 Materials and Preparation

As fumed TiO_2, commercially produced TiO_2 with different surface areas and primary particle sizes, (AEROXIDE® TiO_2 P 25: $50m^2/g$; 21nm; (P25), AEROXIDE® TiO_2 P 90: $90m^2/g$;14nm; (P90) and sample A: $65m^2/g$;18nm;　produced by Nippon AEROSIL Co., Ltd.) were used. An electric tubular furnace (OSK 55DB125B Ogawa Seiki Co., Ltd.) was vertically placed and equipped with a 2 L glass conical beaker at the bottom with a wrapped opening by oven cloth to protect the upstream inserted air. A sample of TiO_2 was directly dropped from top of the furnace to the bottom by a natural dropping method without a sieve or through several mesh sizes of sieves (0.5mm, 1.0mm and 1.4mm) fixed on the top of the electric furnace. The sieve was vibrated by a vibration device (THRIVE HandyVibe MD-01 Daito Electric Machine Industry Co., Ltd.). The electric furnace was heated at several temperatures from 800 ℃ to 1450 ℃. The thermal treatment time was measured by checking the dropping time of the fumed TiO_2 from the top to the bottom by visual inspection. A schematic outline of experimental apparatus for thermal treatment is illustrated in Fig. 1.

2.2 Characterization

The crystalline phases were analyzed by an X-ray diffractometer (XRD-6100 Shimazu Corp.) using Cu-Kα radiation to identify the content of rutile and anatase of the thermally-treated fumed TiO_2. The content of rutile (f rutile) was calculated by using the following equation [17].

f rutile = 1 − f anatase ;

f anatase = 1/ (1 + 1.26 (I rutile / I anatase))

I rutile, I anatase: XRD peak intensity of rutile (110) and anatase (101) structure

The particle size distribution was measured by a MT3300EX2 from the MicrotracBEL Corp. The surface area was measured by the BET technique (Macsorb HM-1200S Mountech Co., Ltd.) using the one point measurement method [18].

For the sedimentation test, 0.5 wt. % of a TiO_2 water dispersion was prepared by an ultrasonic homogenizer (US-300CCVP Nihon Seiki Kaisha, Ltd.,) at 300 W for 5 minutes. The resulting dispersion was poured into a 15 ml sedimentation tube graduated on the outside of the wall. One ml of the dispersion was taken from the 8-ml point of the sedimentation tube and the absorbance of the water dispersion was measured by a spectrophotometer (V-670 JASCO Corp.) at a 700 nm light wavelength. The appearance of the water dispersion in the sedimentation tube was also visually observed. The water vapor adsorption-desorption isotherms were measured by a BELSOP-max (MicrotracBEL Corp.). The nanostructure and morphology were observed by a transmission electron microscope (TEM, JEM-1010 JEOL Ltd.).

3. Results and Discussion

3.1 Conversion ratio from anatase to rutile structure

Table-1 is a summary of the results of the thermal treatment of P25 at 1450 ℃ without the sieve and through the 0.5mm mesh sieve. The original P25 has the content of rutile (15%). After the thermal treatment at 1450 ℃ without the sieve, P25 showed a slight increase in the content of rutile (from 14 % to 16 %). However, by passing the sample through the 0.5mm mesh sieve, there was a drastic increase in the content of rutile (from 14 % to 94 %). The thermal treatment time was measured at less than 1 second in both cases.

Fig.2 shows the X-ray diffraction (XRD) peaks of the anatase (101) and rutile (110) for the P25 treated at several temperatures through the 0.5mm mesh sieve. In all cases, the thermal treatment time was less than 1 second. The XRD data indicated that the content from anatase to rutile (%) was significantly affected by the temperature rise. The anatase gradually decreased depending on the increase in the thermal treatment temperature and the content of rutile (%) increased relative to the anatase.

Fig. 3 confirms the content of rutile for three fumed TiO_2 samples with different surface areas treated at several temperatures from 800 ℃ to 1450 ℃ through the 0.5mm mesh sieve. P90 and Sample A indicated higher content of rutile than P25 for the same thermal treatment temperature and they showed the content of rutile around 100 % when prepared at 1450 ℃. The surface area of the fumed TiO_2 is directly related to its primary particle size. These two fumed TiO_2 more easily transform from anatase to rutile than P25 because of their small primary particle size.

In regards to the mesh size of the sieve, there is a border in mesh size between 1.0mm and

1.4mm. High content of rutile was obtained by passing the material though less than the

1.0mm mesh sieve. When the 1.4 mm mesh sieve was applied, the content of rutile was much

lower than that of the 0.5mm and 1.0 mm mesh sieves. As examples, for a thermal treatment

at 1450 ℃, P25 showed the content of rutile (94 %) for both the 0.5mm and 1.0mm, and 73%

under 1.4mm. P90 was confirmed to have the content of rutile (over 97%) under both 0.5mm

and 1.0mm, and 74% under 1.4mm.

These results suggest that small agglomerate size is preferred for the transformation using this

natural dropping method penetrating the thermal energy into the entire agglomerate due to

very short thermal treatment time.

3.2 Surface area

Fig. 4 displays the surface area ($S._{BET}$) of the fumed TiO_2 from 800 to 1450 ℃ using the 0.5mm

mesh sieve. It is evident that a decrease in surface area is observed in all cases. Especially,

Sample A and P90 show lower surface areas than P25 for the same thermal treatment

temperature over 1100 ℃. These surface area data demonstrate the reversed results of the

conversion ratio of rutile shown in Fig.3. It is assumed that sintering and grain growth of the

particles in these two fumed TiO_2 progress faster than P25 due to their small primary particle

sizes.

3.3 Dispersibility

The particle size distribution of the thermally-treated P25 at 1450 ℃ through the 0.5mm mesh sieve was measured and compared to the other types (Chloride process) of TiO_2 (Sample B: CR-EL (7m2/g) Ishihara Sangyo Co. Ltd.,) with the rutile structure and similar surface area as a reference. Fig. 5 confirms the particle size distribution, (a) without ultrasonic irradiation and (b) ultrasonic irradiation at 40 W for 3 minutes. Without ultrasonic irradiation in Fig.5 (a), the main peak of the thermally-treated P25 appears around 200μm and it indicates very wide range from 1μm to 1000μm. The main peak of Sample B appears around 1.8μm with a narrower particle size distribution than the thermally-treated P25. When the ultrasonic irradiated at 40 W for 3 minutes as shown in Fig. 5 (b), the main peak of the thermally-treated P25 shifts to a lower range. However, it still shows a larger particle size than Sample B. These results indicate that the thermally-treated P25 demonstrates a quite larger particle size and broader particle size distribution than that of sample B.

The absorbance measurement of the water dispersion is an effective method for the evaluation of the dispersibility of the powders in media [19]. Fig.6 indicates the relationships between the absorbance of water dispersion and storage time for both the thermally-treated P25 at 1450 ℃ and Sample B. The thermally-treated P25 has a higher absorbance than Sample B from just after forming the dispersion up to 50 hours storage. This absorbance is directly related to the transparency of the water dispersion. This result suggests that the thermally-treated P25 has a slower sedimentation speed and higher dispersibility in the water dispersion than Sample B although it displays a larger particle size than Sample B based on the particle size distribution

measurement.

The photos of the dispersion of both the thermally-treated P25 and Sample B in the sedimentation test are illustrated in Fig.7. It is clear that the water dispersion of the thermally-treated P25 shows a turbid color with a low transparency during 50 hours of storage by visual inspection. On the other hand, it was also observed that the water dispersion of Sample B became clear from the middle to top of the sedimentation tube for less than 7 hours storage. Obviously, the particles of Sample B are easily precipitated.

For estimation of the sedimentation velocity, the Stokes's equation was used. By applying the 1 μm diameter Sample B particles measured by the particle size distribution shown in Fig.5.(b) to the Stokes's equation, a 0.56 cm/hour sedimentation velocity was obtained. This result shows a relatively good consistency with the result of the sedimentation test for Sample B.

On the other hand, for the thermally-treated P25 at 1450 °C, by applying a 2 μm diameter shown in Fig.5.(b), a 2.2 cm/hour sedimentation velocity was obtained.

This calculation result is quite different from the current sedimentation result, and in fact, a totally opposite result. From the Stokes's equation, not only the particle size, but also the particle density influenced the sedimentation velocity. This difference suggested that the thermally-treated P25 has a much lower powder density even though it has a larger average particle size than Sample B. The thermally-treated P25 contains many pores in the agglomerate.

3.4 The nanostructure and morphology

It is well known that vapor adsoption-desoprtion isotherm is an effective method for characterizing the nanostructure and morphology of porous particles. Water vapor is selected as the measurement vapor of it because it can detect micro pores based on smaller molecular size than nitrogen. [20]   For the fine powders produced by the fumed process, water vapor was applied to characterize nanostructure of both the original core particles and surface modified ones. [21-23].

Fig.8 shows the water adsorption-desorption isotherms for the original and thermally-treated P25 at 1450 ℃. The original P25 exhibits a type-Ⅱ isotherm according to the BDDT classification. This   result   is   different   from   the result of the fumed silica, which shows a type-Ⅲ isotherm [24],   although   both   oxides   are   produced   by   the   same fumed process. However, the thermally-treated P25 at 1450 ℃ exhibits a different type of isotherm, i.e., a type-IV isotherm with hysteresis loops, in the higher pressure range from 0.5 to 0.9.

It is known that the hysteresis loop in this range is due to mesopores. The thermally-treated P25 at 1450 ℃ confirms this hysteresis although the original P25 does not show it. This result indicated that the thermally-treated P25 contains many pores made by closing the open pores by partial sintering between the particles. Some pores made by small particles act like pseudo-mesopores. Based on this characterization, the thermally-treated P25 acts like a pseudo-large particle during the measurement of the particle size distribution. It has low density particles

and shows a low sedimentation velocity and high dispersibility in the water dispersion test. Furthermore, water would be able to enter some of the large pores by strong ultrasonic irradiation when it was dispersed in the water.

The average crystal size of the fumed TiO_2 (D in nanometers) can be estimated by Scherrer's equation.

$$D = 0.89*\lambda / B(2\theta)*\cos\theta$$

λ: X-ray wavelength (nanometer),

B(2θ): width of the XRD peak at half-peak height in radians,

θ: angle of diffracted peak in degrees.

The crystal size of the original P25 was estimated to be around 20nm from the anatase (101) and 26nm from rutile (110) diffraction peaks. On the other hand, the crystal size of the thermally-treated P25 at 1450 ℃ was estimated to be around 20nm from anatase (101) and 32nm from the rutile (110) diffraction peaks. These results indicated that crystal size growth of rutile occurred at the same time during transformation from the anatase to rutile. This crystal size growth also results in grain growth of the particles.

Fig.9 illustrates the image scheme and the porous-type of morphology. Thermally-treated P25 transforms from anatase to rutile and crystal size growth occurs even though short thermal treatment time. It contains two type of pores in the agglomerate. One is a normal type of pore and another is a small type of pore. The normal type of pore is made by closing of the open spaces of pores in P25 agglomerate with the connection of normal and large sized of particles

by the partial sintering. On the other hand, small type of pore is made by closing of the open pores among small particles by the partial sintering. These small pares act like pseudo-mesoporous type of phenomena. Thermally-treated P25 also exhibits pseudo-large particles in the particle size distribution measurement. Each particles are connected partially and make large particles in appearance containing many porous. The transmission electron microscope images of the thermally-treated P25 at 1450 ℃ are shown in Fig.10. The connections of each particle by partial sintering and grain growth are observed in the agglomerate and they formed many pores in the agglomerate. These results support the formation of a porous-type of fumed TiO_2.

There are several studies related to the porous or mesoporous TiO_2. Some of them are related to the photocatalytic activity of the TiO_2 coating made by the sol-gel process [25-26]. The porous-type of morphology in this study is different from these previous studies.

4. Conclusions

In summary, the fumed TiO_2 powder with a high content of rutile (97%) was successfully synthesized by a novel thermal treatment for the transformation from the anatase to the rutile structure. The natural dropping method was used for the production process in order to reduce the thermal treatment time. The thermally-treated TiO_2 confirmed the high dispersibility in the water dispersion and type-IV isotherm with hysteresis loops in the water adsorption-desorption isotherms. These results suggest that many open pore spaces of the

agglomerated P25 would be partially closed by partial sintering of the particles of the agglomerate and it makes a porous-type of morphology.

5. Acknowledgments

6. References

[1] Xiaobo Chen and Samuel S. Mao, Titanium Dioxide Nanomaterials: Synthesis, Properties, Modifications, and Applications. Chemical Reviews, 107(7) (2007) 2891-2959

[2] Degussa. Titanium Dioxides P25 Manufacture-Properties-Applications, Technical Bulletin Fine Particles, 80 (2003) 1-26

[3] S. Deguchi, N. Shibata, T. Takeichi, Y. Furukawa and N. Isu, Photocatalytic Hydrogen Production from Aqueous Solution of Various Oxidizing Sacrifice Agents. J. Japan Petroleum Institute, 53 (2) (2010) 95-100.

[4] Y. Suyama and A. Kato, Mechanism of Action of Additives on Anatase-Rutile Transformation. Zairyo, 27 (298) (1978) 632-637.

[5] S.V. Zaitsev, J. Moon, H. Takagi and M. Awano, Preparation and characterization of nanocrystalline doped TiO_2. Adv. Powder Technol. 11(2) (2000) 211-220.

[6] Y. Suyama and A. Kato, The Inhibitory Effect of SiO_2 on the Anatase-Rutile Transition of TiO2. Yogyo-Kyokai-Shi, 86 (3) (1978) 119-125.

[7] M. Inagaki, Suppression of Phase Transformation in Titanium Dioxide by Carbon Coating. Aichi Institute of Technology Bulletin of Research Institute for Industrial Technology, 9 (2007) 67-71.

[8] B. Ahmmad, Y. Kusumoto and Md. S. Islam, One-step and large scale synthesis of non-metal doped TiO2 submicrospheres and their photocatalytic activity. Adv. Powder Technol. 21 (2010) 292-297.

[9] K. Prasad a, D.V. Pinjari, A.B. Pandit, S.T. Mhaske, Phase transformation of nanostructured titanium dioxide from anatase-to rutile via combined ultrasound assisted sol-gel technique. Ultrasonics Sonochemistry, 17 (2010) 409–415.

[10] S. Kittaka, K. Matsuno, and S. Takahara, Transformation of Ultrafine Titanium Dioxide Particles from Rutile to Anatase at Negatively Charged Colloid Surfaces. J. Solid State Chemistry 132 (1997) 447-450.

[11] T. Wakamatsu, T. Fujiwara, K. N. Ishihara and P. H. Shingu, Formation of Brookite-Type TiO_2 Titania by Mechanical and Alloying. J. Japan Society of Powder and Powder Metallurgy. 48 (10) (2001) 950-954.

[12] Y. Ikuma and T. Shigemura, Rapid-Rate Sintering of Anatase-Type TiO_2 by Microwave Heating. J. Ceramic Society of Japan 101 (8) (1993) 900-904.

[13] Y. Suyama and A. Kato, Sintering of Fine TiO_2 Powders Prepared by Vapor-phase

Reaction. Yogyo-Kyokai-Shi,89 (3) (1981) 140-147.

[14] K. Hijikata, Sintering of Oxides – Effect of Atmosphere. J. Japan Society of Powder and Powder Metallurgy, 18 (5) (1972) 163-174.

[15] M. Asano and T. Taniguchi, Photocatalytic Effect of Anatase-TiO_2 Polycrystalline Prepared by Normal Sintering. Report of Nara Prefectural Institute of Industrial Technology, (26) (2000) 27-31.

[16] J.F. Porter, Y-G. Li and C. K. Chan, The effect of calcination on the microstructural characteristics and Photoreactivity of Degussa P-25 TiO2, J. Materials Sci., 24, (1999) 1523-1531.

[17] R. A. Spurr, H. Myers, Quantitative Analysis of Anatase-Rutile Mixtures with an X-ray Diffractometer. Anal. Chem., 29 (1957) 760-762.

[18] Determination of the specific surface area of powders (solids by gas adsorption-BET method. JIS Z8830 (2013) 1-24.

[19] Y. Mitani, T. Teshima, Y. Yoshida and N. Yamazoe, Dispersibility of Fumed Silica in Simple Media. J. Ceramic Society of Japan 101 (6) (1993) 707-712.

[20] **H. Naono, Characterization of Powder by Adsorption of Nitrogen Gas and Water Vapor. J. Powder Tech. Soc. Jpn.,28 (1) (1991) 34-39.**

[21] M. Fuji, H. Iwata, T. Takei, T. Watanabe and M. Chikazawa, The change in the water vapor affinity of fine silica particles loaded with trimethylsilyl groups. Advanced Powder Technol., 8(4) (1997)325-334.

[22] M. Fuji, H. Iwata, T.Takei, T. Watanabe and M. Chikazawa, The Change in Wettability

and Structure of Silica Powder Surfaces Modified with Hexamethyldisilazane. J. Soc. Powder Technol., Japan, 33 (1996) 740-746.

[23] M. Fuji, H. Iwata, T.Takei, T. Watanabe and M. Chikazawa, The Change in the Water Vapor Affinity of Fine Particles Loaded with Trimethylsilyl Group. J. Soc. Powder Technol., Japan, 32 (1995) 649-654.

 [24] M. Fuji, H. Iwata, T. Takei, T. Watanabe and M. Chikazawa, The change in the water vapor affinity of fine silica particles loaded with trimethylsilyl groups. Advanced Powder Technol., 8(4) (1997)325-334.

[25] J. Yu, X. Zhao, J. Du and W. Chen. Preparation, Microstructure and Photocatalytic Activity of the Porous TiO_2 Anatase Coating by Sol-Gel Processing. J. Sol-gel Science and Technol., 17 (2000) 163-171.

[26] M. Zhou, J. Yu, B. Cheng and H. Yu, Preparation and photocatalytic activity of Fe-doped mesoporous titanium dioxide nanocrystalline photocatalysts, Materials Chemistry and Physics, 93 (2005) 159-163.
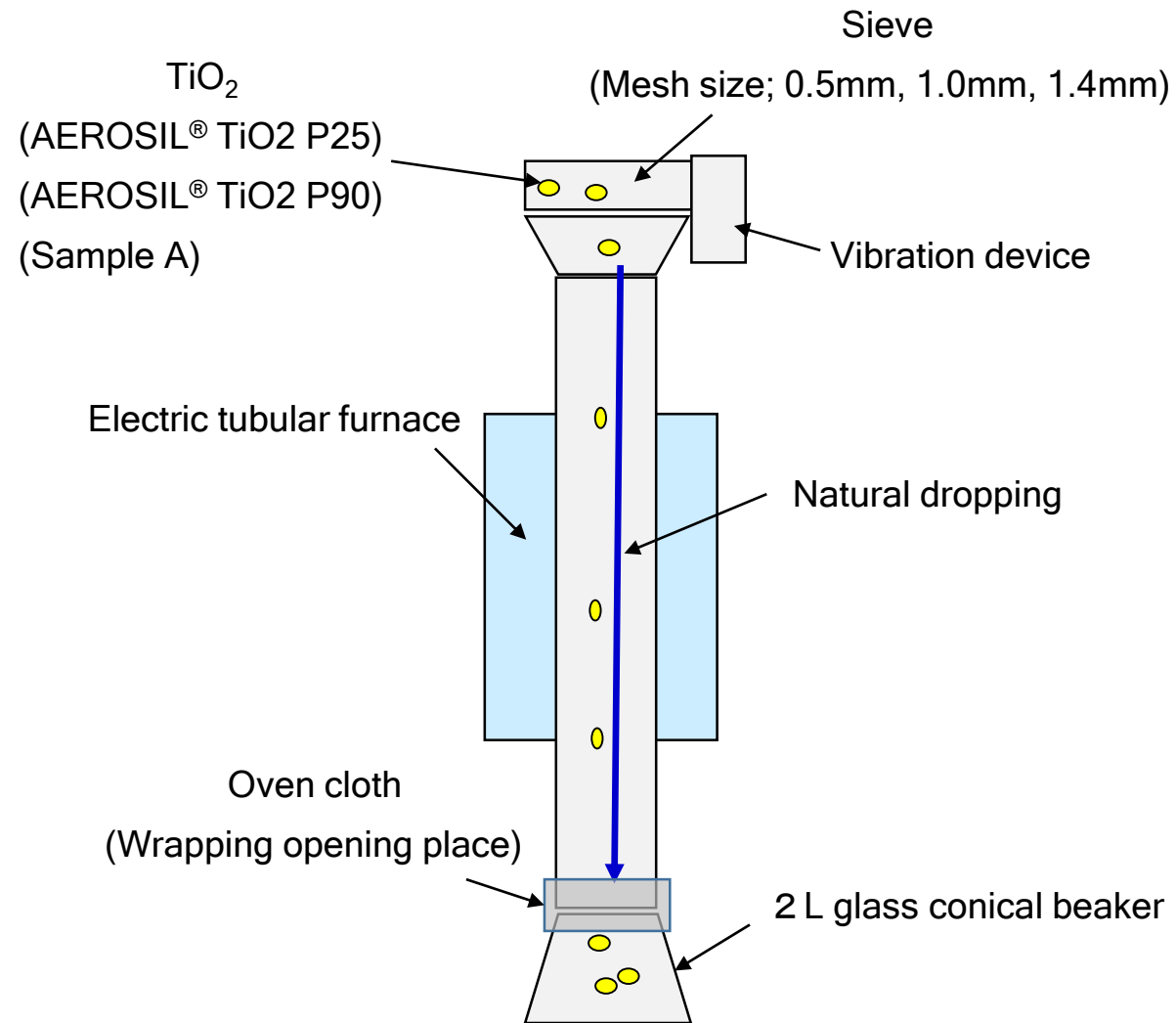
Fig.1. Schematic outline of experimental apparatus for thermal treatment
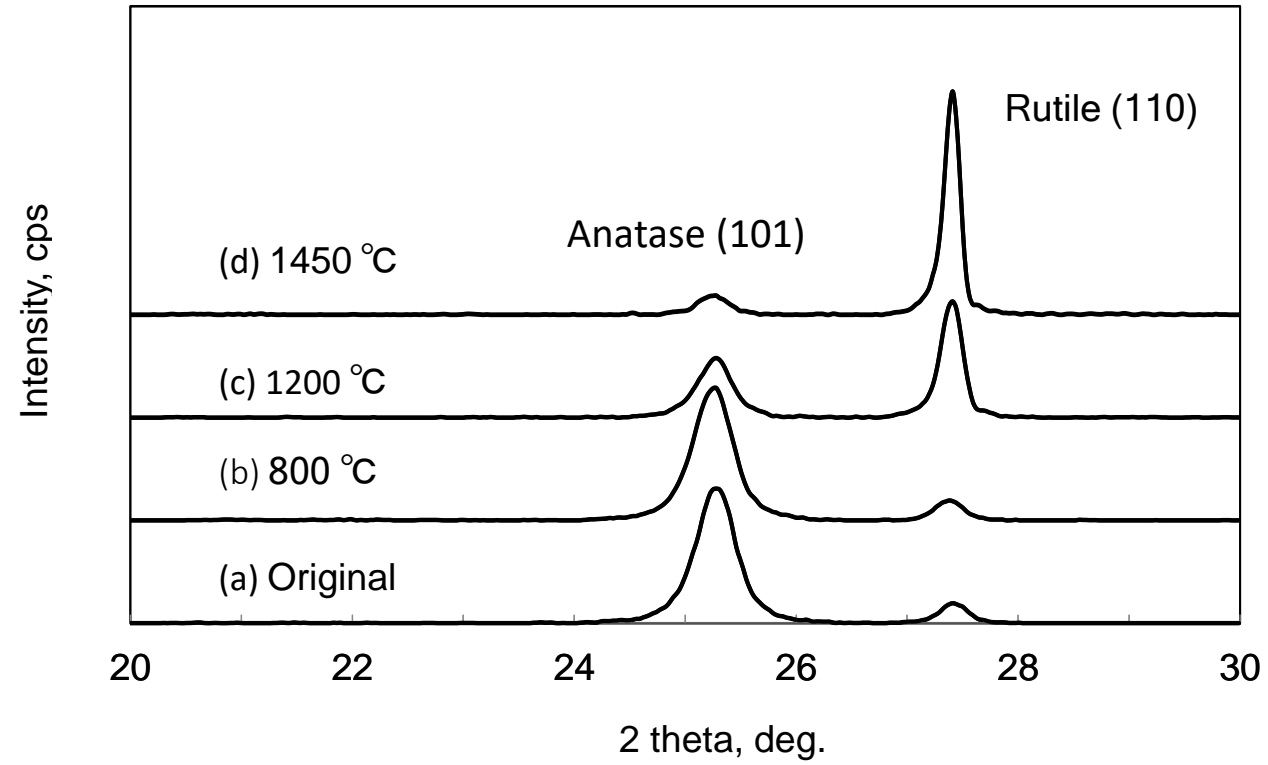
Fig. 2. XRD patterns of thermal treated P25
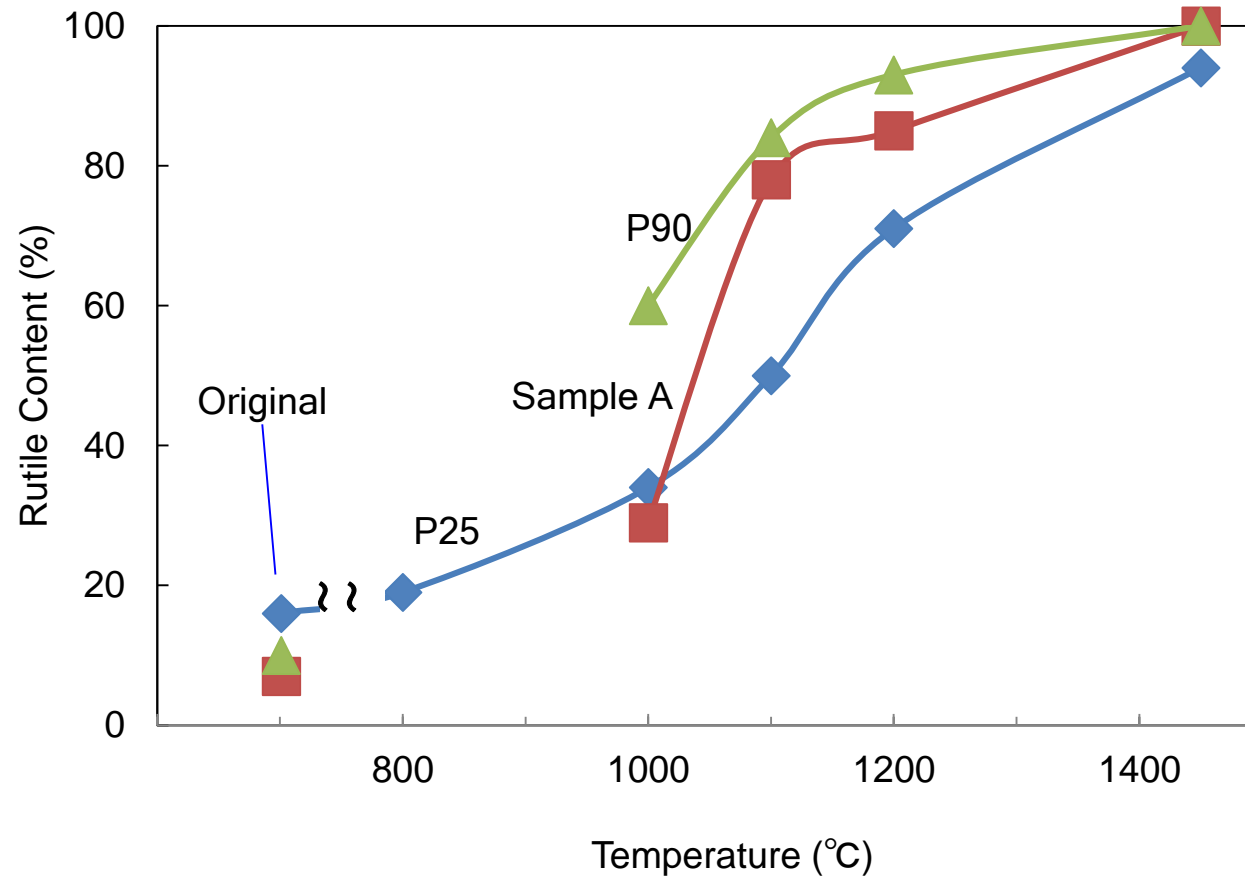
Fig. 3. Rutile conversion ratio of thermal treated fumed TiO_2
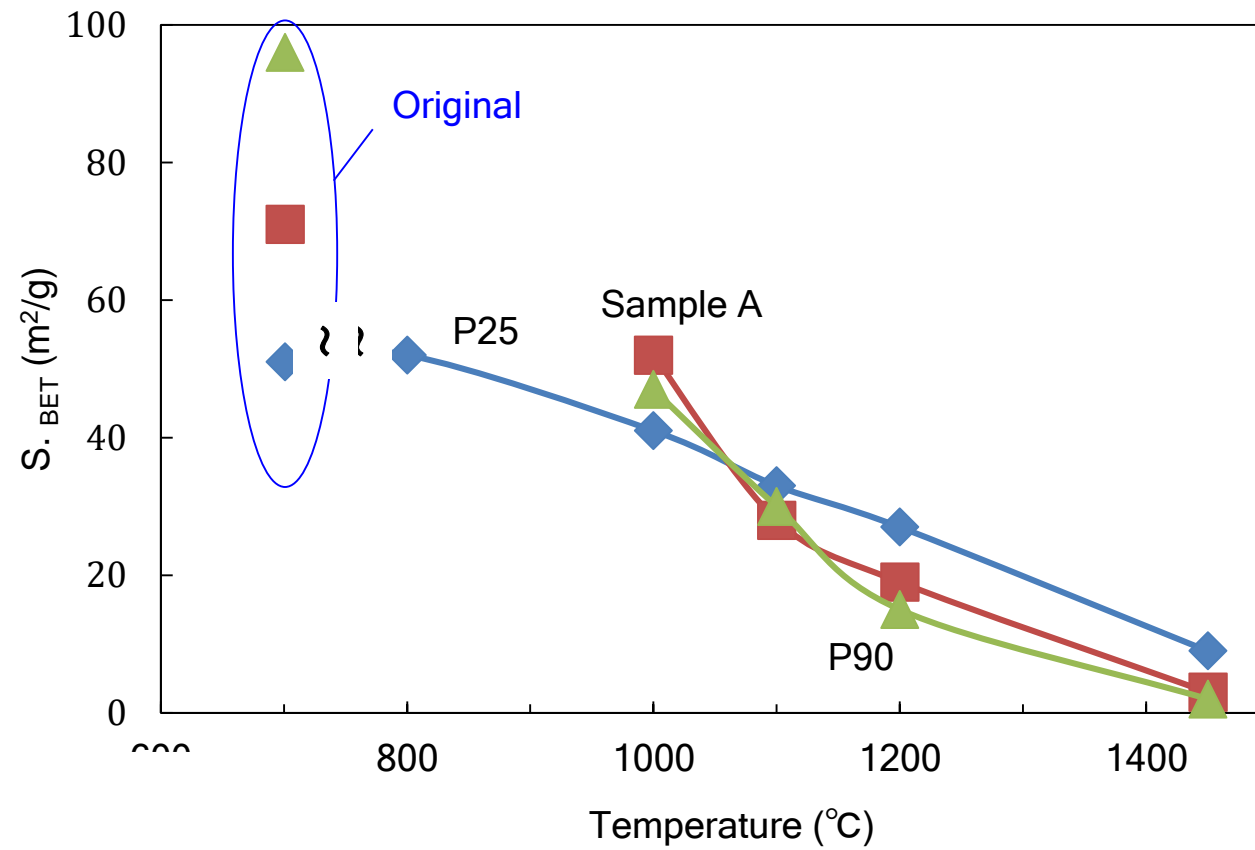
Fig. 4. Surface area of thermal treated fumed TiO$_2$
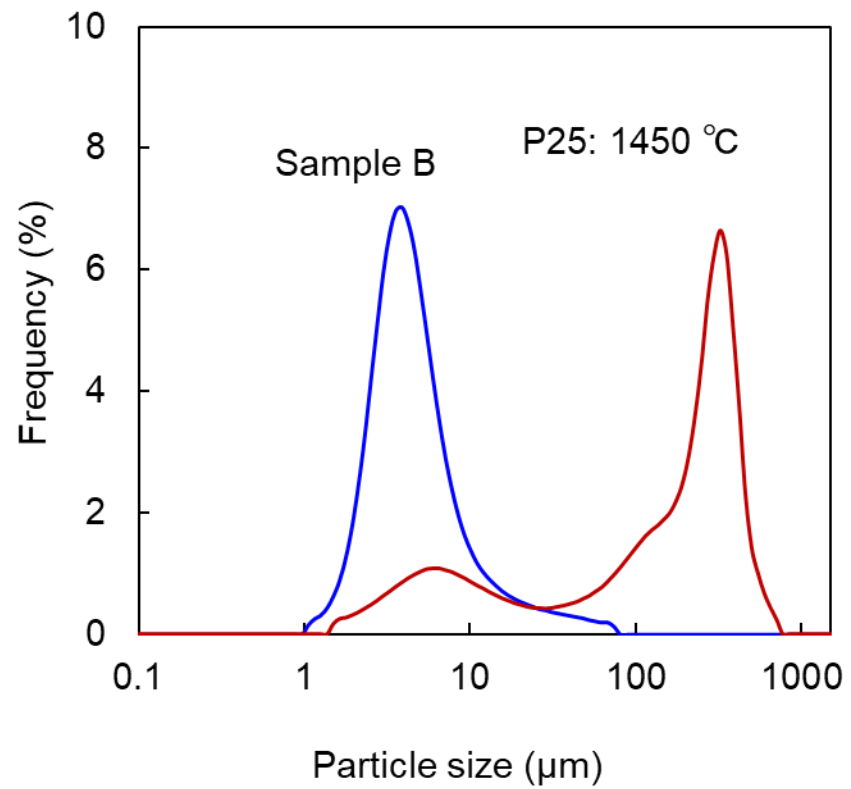
(a) Without Ultrasonic irradiation
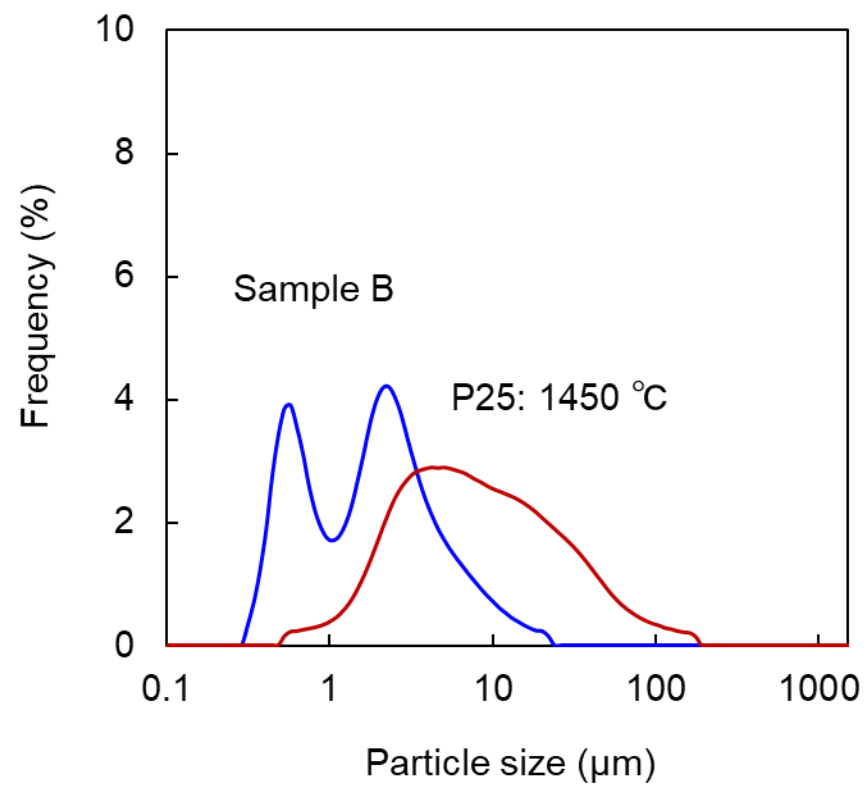
(b) Ultrasonic irradiation 40W 3 minutes

Fig. 5. Particle size distribution of TiO_2
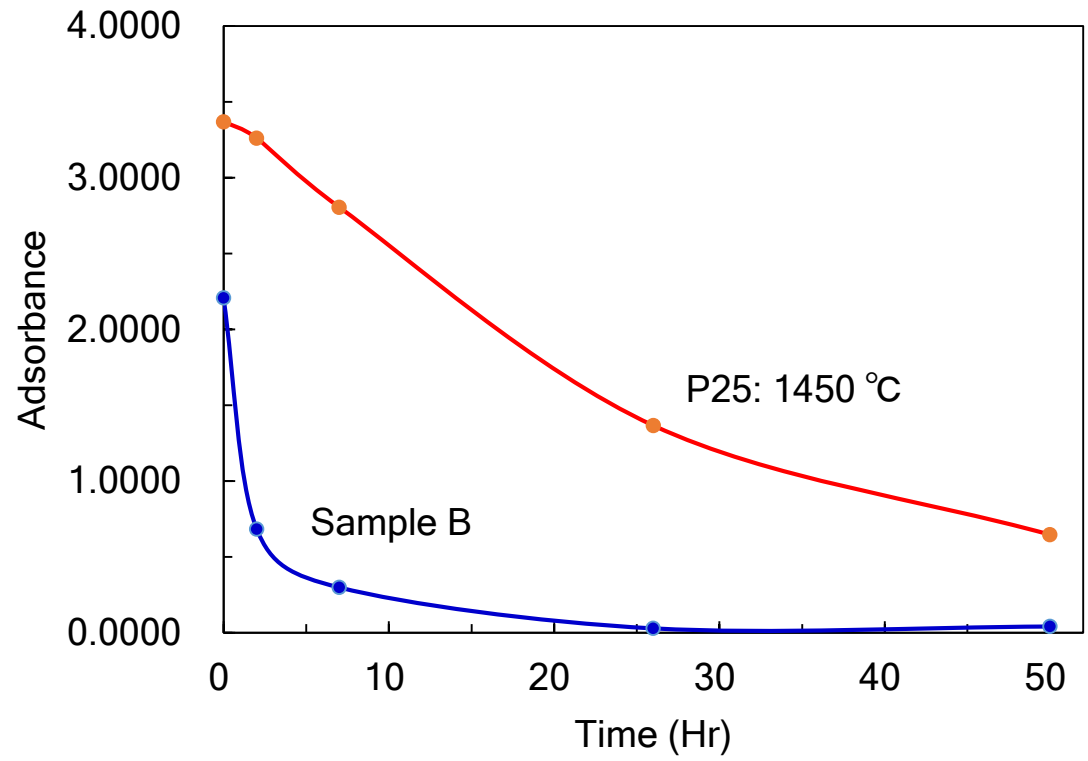
Fig. 6. Absorbance of TiO$_2$ water dispersion
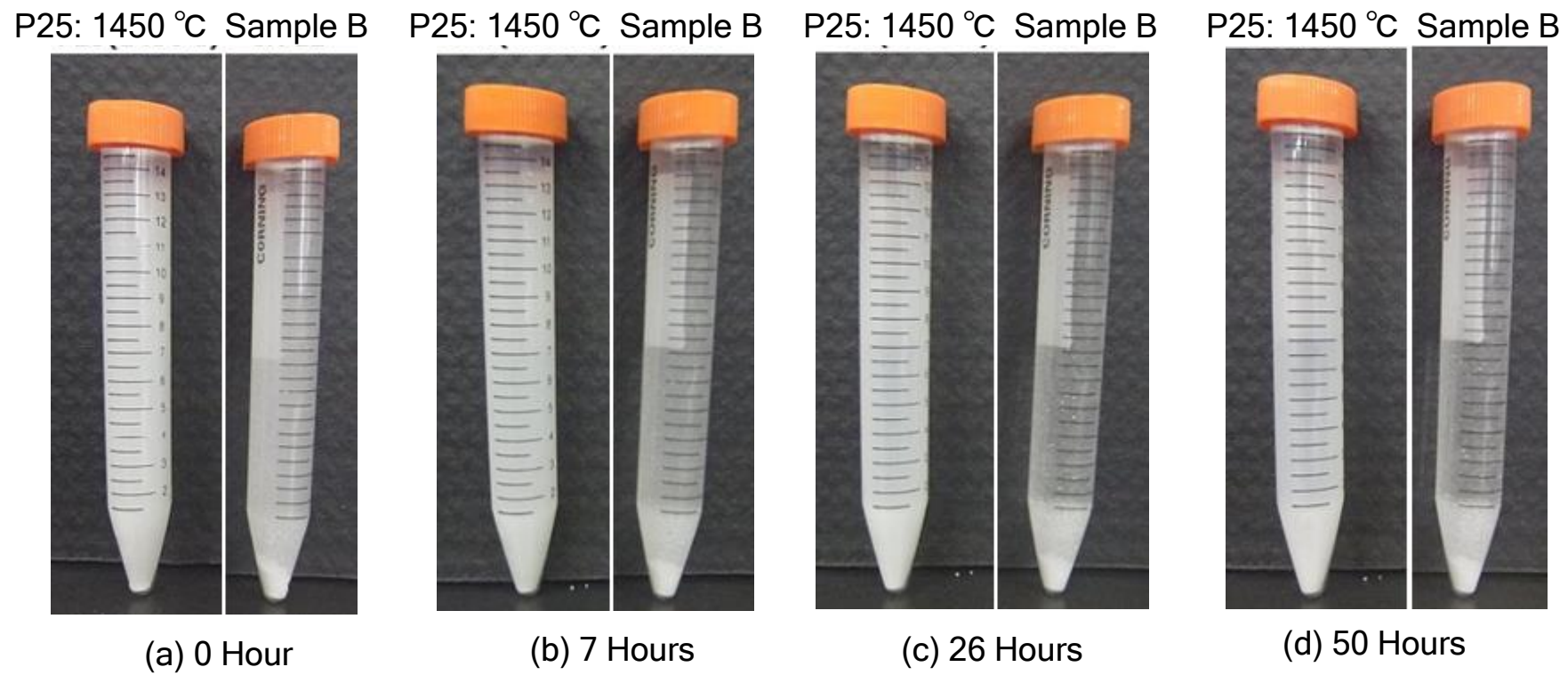
Fig. 7. Photos of TiO_2 water dispersion for the sedimentation test
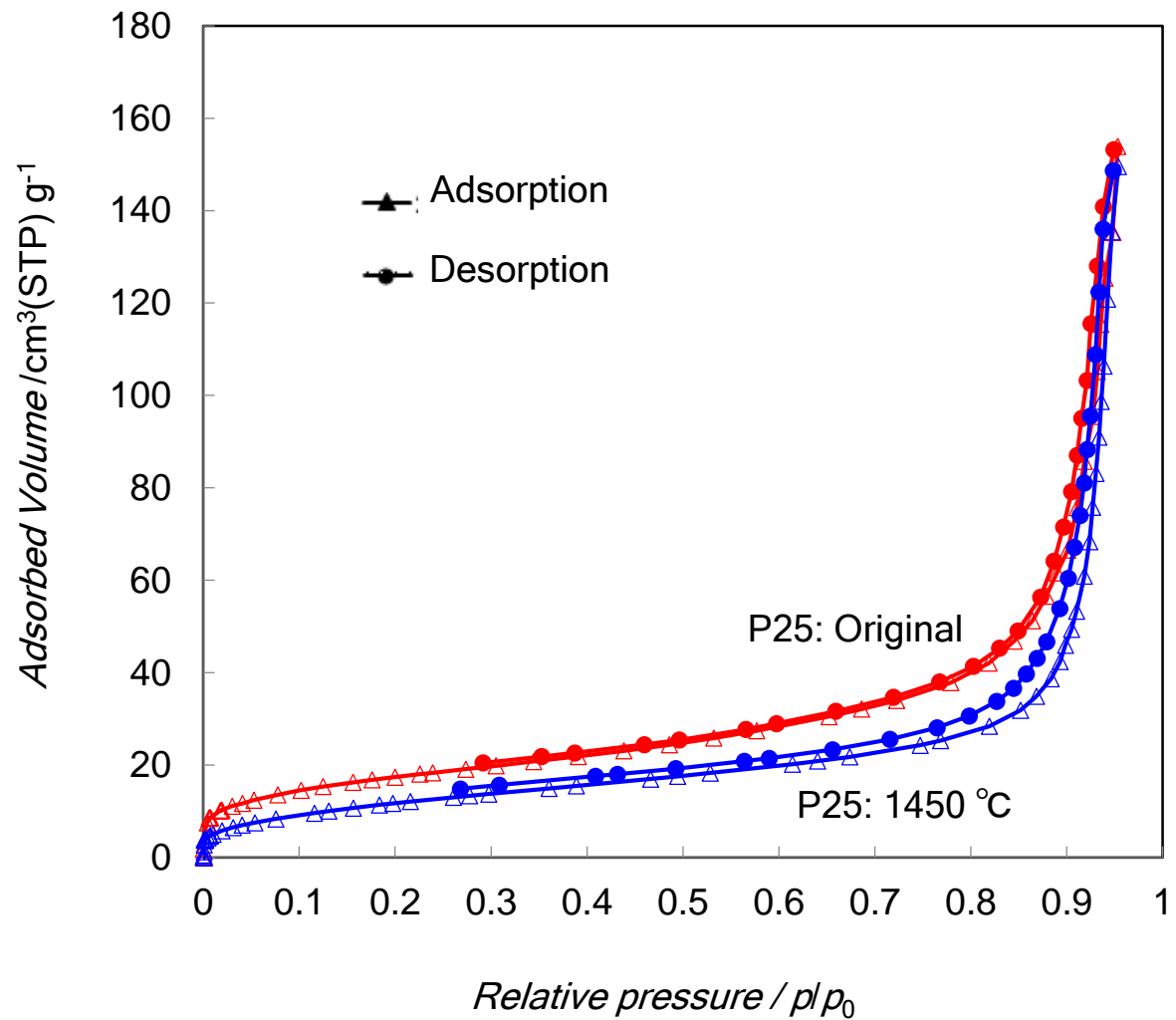
Fig. 8. Adsorption / Desorption curves of P25
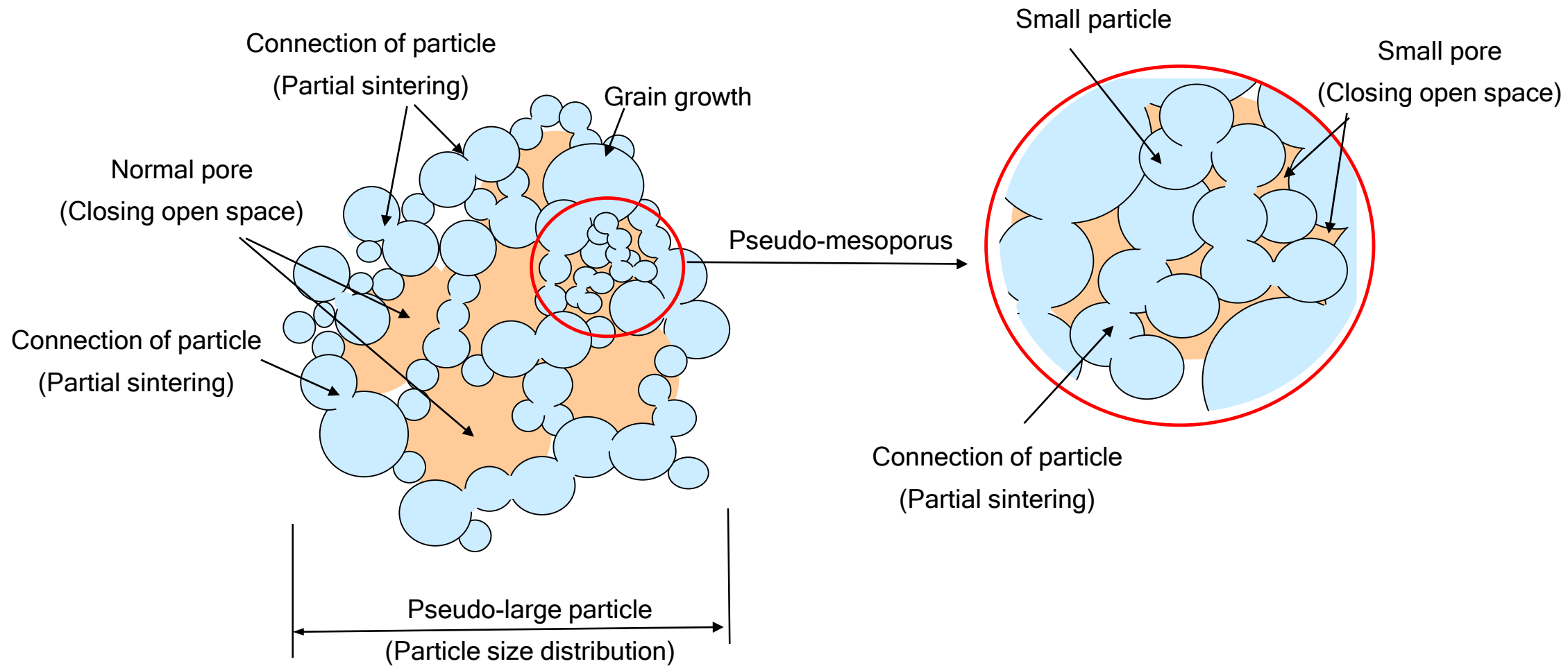
Fig. 9. Image of porous-type of fume TiO_2
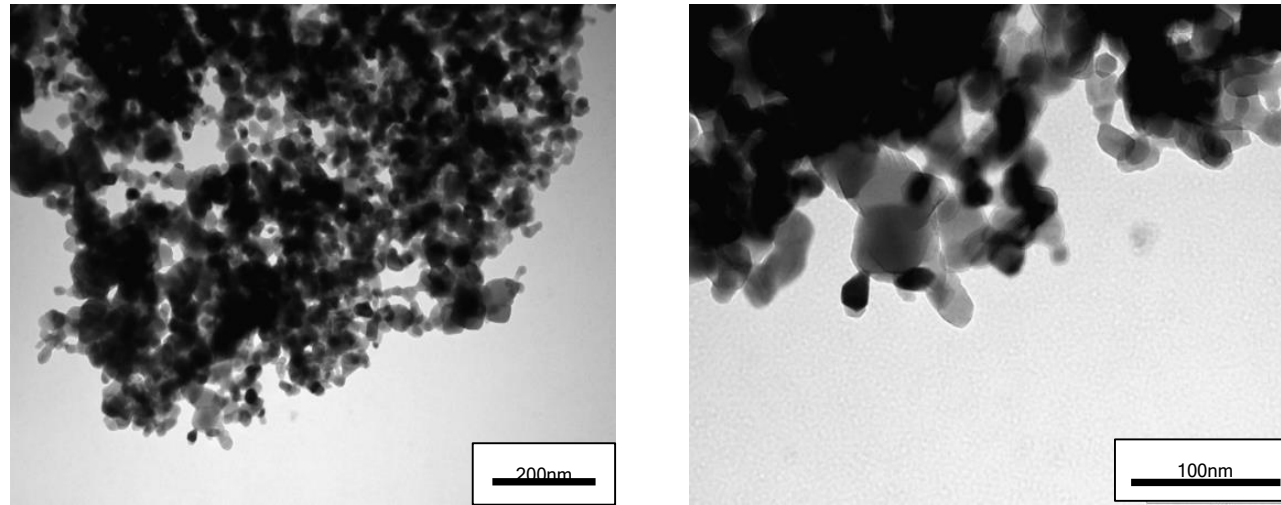
Fig. 10. Transmission electron image of thermal treated P25

Table 1

Physical properties of P25 after thermal treatment

Temperature (℃)	Mesh size of sieve (μ m)	Rutile ratio (%)	S_{BET} (m^2/g)
Room temperature	-	16	51
1450	-	18	49
1450	500	94	9